

# Particles with Coordinated Patches or Windows from Oil-in-Water Emulsions

Young-Sang Cho,<sup>†</sup> Gi-Ra Yi,<sup>‡</sup> Shin-Hyun Kim,<sup>†</sup> Seog-Jin Jeon,<sup>†</sup> Mark T. Elsesser,<sup>§</sup>  
Hyung Kyun Yu,<sup>†</sup> Seung-Man Yang,<sup>\*,†</sup> and David J. Pine<sup>§</sup>

National Center for Integrated Optofluidic Systems and Department of Chemical and Biomolecular Engineering, Korea Advanced Institute of Science and Technology, Daejeon 305-701, Korea, Nano-Bio System Research Team, Seoul Center, Korea Basic Science Institute, Seoul 136-713, Korea, and Department of Physics, New York University, New York, New York 10003

Received January 8, 2007. Revised Manuscript Received April 6, 2007

In this paper, we demonstrated a unique and simple method for fabricating colloidal particles of complex structures using oil-in-water emulsion droplets as confined geometries. A variety of structural motifs were produced using binary colloids of microspheres of polystyrene (PS) or silica and nanosized particles as the second component. When PS or silica microspheres and PS macromolecules were dispersed in oil-in-water emulsion droplets, particles with well-coordinated patches were obtained because the PS macromolecules partially covered the microsphere clusters. When silica or gold nanoparticles were dispersed together with the PS microspheres in oil-in-water emulsion droplets instead of PS macromolecules, composite particles with patches were obtained. In this case, silica or gold shell structures with well-coordinated windows were produced by selectively removing the large PS microspheres from the organic–inorganic composite clusters.

## Introduction

The packings of microspheres have attracted great attention in materials physics and chemistry for their potential applications as complex materials with desired functionalities. Over the past decades, various methodologies have been developed for fabricating the suprastructures of a large number of microspheres such as colloidal crystals and complex surface patterns.<sup>1,2</sup> Recent development of colloidal molecules or patchy particles, which are regularly structured aggregates of colloidal microspheres, has materialized two- or three-dimensional complex colloidal structures with unique physicochemical properties or helped us to understand fundamental physics of complex colloids.<sup>3</sup> Moreover, complex colloids have been proposed for various applications such as photonic molecules for tight binding photon devices and sensors and mirrorless microlasing.<sup>4,5</sup> Recently, Manoharan et al.

developed a convenient and robust method for preparing small clusters of microspheres from toluene-in-water emulsion droplets. In their process, polystyrene (PS) microspheres encapsulated in toluene droplets were packed into clusters during the slow evaporation of toluene.<sup>6</sup> The configurations of the PS microsphere clusters were unique, minimizing the second moment of the particle mass distribution up to  $n = 11$ , in which  $n$  is the number of the constituent microspheres. The second moment of the particle distribution is defined as

$$M = \sum_{i=1}^n |r_i - r_0|^2$$

in which  $r_i$  is the position of  $i$ -th sphere and  $r_0$  is the center of mass of the cluster. By density gradient centrifugation, the PS microsphere clusters could be fractionated successfully, which produced all-identical small clusters of unique configurations depending only on the number  $n$  of the constituent particles. More recently, we also reported a similar pathway for cluster formation using phase-inverted water-in-oil emulsion, which is useful for the colloids that are more stable in aqueous media rather than oil phase.<sup>7</sup> In spite of these advances, it still remains a contemporary challenge to fabricate colloidal clusters with multicomponent and multifunctional materials. In particular, the controlled arrangement of conducting microspheres and semiconducting nanoparticles of different compositions can open a new

\* Corresponding author. E-mail: smyang@kaist.ac.kr.

<sup>†</sup> Korea Advanced Institute of Science and Technology.

<sup>‡</sup> Korea Basic Science Institute.

<sup>§</sup> New York University.

- (1) (a) Caruso, F. *Colloids and Colloid Assemblies: Synthesis, Modification, Organization and Utilization of Colloid Particles*; Wiley-VCH: Weinheim, Germany, 2004. (b) Ramos, L.; Lubensky, T. C.; Dan, N.; Nelson, P.; Weitz, D. A. *Science* **1999**, *286*, 2325. (c) Velev, O. D.; Lenhoff, A. M.; Kaler, E. W. *Science* **2000**, *287*, 2240. (d) Prevo, B. G.; Velev, O. D. *Langmuir* **2004**, *20*, 2099.
- (2) (a) Yang, S.-M.; Jang, S. G.; Choi, D.-G.; Kim, S.; Yu, H. K. *Small* **2006**, *2*, 458. (b) Yin, Y.; Lu, Y.; Gates, B.; Xia, Y. *J. Am. Chem. Soc.* **2001**, *123*, 8718.
- (3) Cho, Y.-S.; Yi, G.-R.; Lim, J.-M.; Kim, S.-H.; Manoharan, V. N.; Pine, D. J.; Yang, S.-M. *J. Am. Chem. Soc.* **2005**, *127*, 15968.
- (4) (a) Reculusa, S.; Poncet-Legrand, C.; Perro, A.; Duguet, E.; Bourgeat-Lami, E.; Mingotaud, C.; Ravaine, S. *Chem. Mater.* **2005**, *17*, 3338. (b) Kim, J.-W.; Larsen, R. J.; Weitz, D. A. *J. Am. Chem. Soc.* **2006**, *128*, 14374.
- (5) Holler, S.; Pan, Y.; Chang, R. K.; Botigger, J. R.; Hill, S. C.; Hillis, D. B. *Opt. Lett.* **1998**, *23*, 1489.

(6) (a) Manoharan, V. N.; Elsesser, M. T.; Pine, D. J. *Science* **2003**, *301*, 483. (b) Manoharan, V. N.; Pine, D. J. *MRS Bull.* **2004**, *29*, 91.

(7) Cho, Y.-S.; Yi, G.-R.; Kim, S.-H.; Pine, D. J.; Yang, S.-M. *Chem. Mater.* **2005**, *17*, 5006.

opportunity for developing colloidal nanotransistors to be addressed individually when they are registered in the lattice by fluidic assembly.<sup>8</sup> Furthermore, for colloids that have well-coordinated sites of directional interactions as molecules do, the colloidal clusters should be covered in part by a partially encapsulating material with exposed patches in designed coordination.

In this article, we demonstrated a unique and simple method for fabricating complex colloids with a variety of structural motifs, which were essentially aggregates of PS or silica microspheres and nanosized particles as the second component. Specifically, when PS or silica microspheres and PS macromolecules were encapsulated in oil-in-water emulsion droplets, complex colloidal clusters with well-coordinated patches were obtained by drying the emulsion droplets. Similarly, composite clusters were prepared using inorganic silica or gold nanoparticles instead of the PS macromolecules. In the latter case, the PS microspheres were burnt out at high temperature or etched out using reactive oxygen ions from the composite clusters, leaving behind inorganic silica or gold architectures with well-coordinated windows. When the emulsion droplets were polydisperse in size, the numbers of the PS microspheres encapsulated in the droplets were nonuniform. Consequently, a variety of the binary colloidal clusters were obtained from a single experiment, which is very useful for understanding the feature of cluster formation. However, it is necessary for practical application to generate monodisperse emulsion droplets and fractionate binary clusters according to their structures, which was also demonstrated in this work. The complex colloids with coordinated patches have directional interactions that are essential for the second self-organization of the patchy particles for novel structures.<sup>8</sup> The hollow silica or gold architectures can be used as catalytic supports, filters, and light diffusers for infrared wavelengths.

## Experimental Section

**Materials.** For cross-linked PS microspheres, styrene monomer (99%), potassium persulfate (initiator, 98%), and sodium hydrogen carbonate (buffer, 99%) were purchased from Kanto Chemicals (Tokyo, Japan) and divinylbenzene (DVB, 80%) was obtained from Aldrich. Another initiator,  $\alpha,\alpha'$ -azodiisobutyramidine dihydrochloride (98%, Fluka) was used for amidine PS particles. Silica microspheres of 1.5  $\mu\text{m}$  in diameter were purchased from Duke Scientific Corp. (Cat No: 8150). Octadecyltrimethoxysilane (OTMOS, 90%), ammonium hydroxide (28%), and chloroform (99.8%) were purchased from Aldrich for surface modification of the silica microspheres. PS homopolymer ( $M_w = 9100$  g/mol) was purchased from Aldrich. Colloidal silica of 30 nm in size dispersed in toluene was purchased from FUSO Chemical Industries (Kyoto, Japan). For colloidal gold, hydrogen tetrachloroaurate(III) hydrate (99.999%), 1-dodecanethiol (98+%), and tetraoctylammonium bromide (98%) were purchased from Aldrich and sodium borohydride (reducing agent, 98%) was obtained from Acros. Toluene (99.8%) and the triblock copolymer of Pluronic F108 [(PEG)<sub>129</sub>-(PPG)<sub>43</sub>-(PEG)<sub>129</sub>] were purchased from Aldrich and BASF, respectively, for generating toluene-in-water emulsion droplets. (**Caution:** toluene is toxic and should be handled with care.) For the density gradient

centrifugation of patchy or composite particles, glycerol (99.5%) and Ficoll type 400 were purchased from MP Biomedicals and Sigma, respectively.

**Synthesis of Cross-Linked PS Microspheres Dispersed in Toluene.** Cross-linked sulfonated PS beads of 230 nm in diameter were prepared by emulsifier-free emulsion polymerization following the procedures in the previous reports.<sup>9</sup> The PS beads were cross-linked by copolymerization of styrene and DVB at 70 °C under vigorous stirring for 10 h using potassium persulfate as an initiator. Cross-linked sulfonated PS microspheres of 830 nm in diameter were synthesized by the seed-growth method using the 230 nm PS beads as seed particles. Similarly, cross-linked amidine PS beads of 400 nm in diameter were prepared by emulsifier-free emulsion copolymerization of styrene and DVB at 70 °C under vigorous stirring for 16 h using  $\alpha,\alpha'$ -azodiisobutyramidine dihydrochloride as an initiator. Cross-linked amidine PS microspheres of 800 nm in diameter were synthesized by the seed-growth method using the 400 nm PS beads as seed particles. Enough DVB was used to prevent the particles from being dissolved in organic solvent such as toluene. For both the seed and final particles, the amounts of DVB used to synthesize sulfonated and amidine PS particles were 5 and 1 wt %, respectively, relative to the amount of styrene. To disperse PS microspheres in toluene, the aqueous suspension of the PS microspheres was washed with ethanol after centrifugation at 3000 rpm. The PS microspheres in ethanol were then redispersed again in toluene after several repeated centrifugations at 3000 rpm in fresh toluene medium. Figure S1 of the Supporting Information shows the SEM images of cross-linked sulfonated or amidine PS microspheres that were synthesized by the seed-growth polymerization.

**Surface Modification of Silica Microspheres.** The silica particles (1.5  $\mu\text{m}$  in diameter) were redispersed in fresh ethanol by centrifugation and redispersion followed by sonication. To disperse silica particles in toluene, the surface of the particles were modified with hydrophobic molecules, OTMOS. Silica dispersion in ethanol (5.1 wt %, 2 mL) was mixed with ammonium hydroxide (0.175 mL) with vigorous stirring. The OTMOS in chloroform (10 vol %, 0.25 mL) was added to the mixture and the reaction proceeded for 2 h. Silica particles were then washed with fresh ethanol and finally redispersed in toluene (2 mL) after centrifugation and redispersion.

**Synthesis of Gold Nanoparticles Dispersed in Toluene.** The 4 nm gold nanoparticles stabilized by dodecanethiol were synthesized by the standard two-phase method.<sup>10,11</sup> Chloroaurate ions were transferred from aqueous hydrogen tetrachloroaurate solution to toluene by a phase transfer reagent, tetraoctylammonium bromide. Dodecanethiol and an excess of the aqueous reducing agent were then added to the solution. After 12 h, two phases were separated and washed with methanol using a membrane filter (molecular weight cutoff: 30 000 Dalton, Millipore Inc.) to remove any unbound dodecanethiol and residual reducing agents. The obtained hydrophobic gold nanoparticles were dried in convection oven at 60 °C and redispersed in toluene at desired concentration by sonication. Figure S2 of the Supporting Information shows the TEM images of 4 nm gold nanoparticles.

**Formation of Patchy or Composite Particles.** The schematic of the preparation of patchy or composite particles is shown in Figure 1. Here, PS or silica microspheres and nanosized second components dispersed in the oil phase were mixed and emulsified

(9) Zou, D.; Aklonis, L. J. J.; Salovey, R. *J. Polym. Sci., Part A* **1992**, *30*, 1463.

(10) Brust, M.; Walker, M.; Bethel, D.; Schiffrin, D. J.; Whyman, R. *J. Chem. Soc., Chem. Commun.* **1994**, *7*, 801.

(11) Brust, M.; Fink, J.; Bethel, D.; Schiffrin, D. J.; Kiely, C. *J. Chem. Soc., Chem. Commun.* **1995**, *16*, 1655.

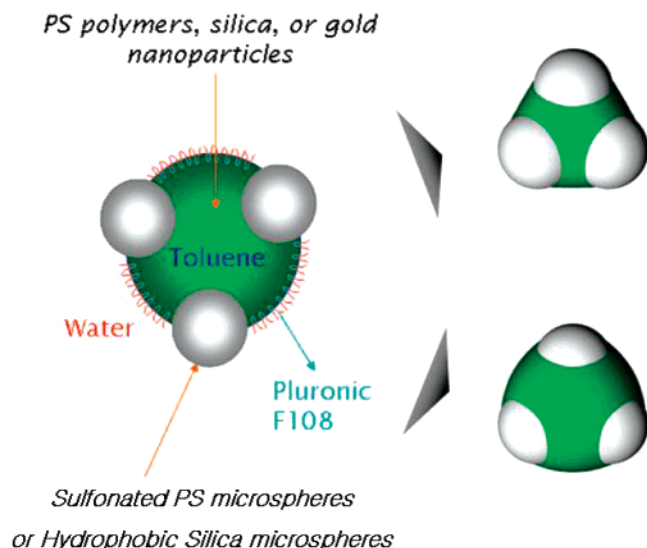


**Figure 1.** Schematic of the fabrication of patchy particles from oil-in-water emulsions by evaporation-induced self-assembly of binary colloids.

in water and binary colloids were then self-organized spontaneously by slow evaporation of the oil-in-water droplets. During the evaporation of the oil phase, capillary forces caused the microspheres and nanosized second components to contact closely and finally to rearrange the configurations of the microspheres after the critical packing.<sup>12</sup> The van der Waals force between the microspheres then cemented the configurations of the composite clusters. Complete evaporation of the oil phase produced small complex structures that were essentially binary colloidal aggregates of microspheres and nanosized particles or macromolecules.

Polymeric patchy particles were produced from toluene-in-water emulsion droplets, which contained sulfonated PS or silica microspheres and PS homopolymers. First, the PS homopolymers were dissolved in toluene by mixing linear PS chains in toluene bath on hot plate at 70 °C for 1 h. Next, a 1 mL suspension of 830 nm PS microspheres (1.8 wt %) in toluene was mixed with 1 mL of a PS homopolymer solution (0.4 wt %) in toluene. The mixture was poured into 16 mL of distilled water with an emulsion stabilizer (1 wt %, Pluronic F108) and emulsified by shearing at 8000 rpm for 60 s. The resulting toluene-in-water emulsion droplets were about 5  $\mu\text{m}$  in average diameter with a polydisperse size distribution ranging from 1 to 10  $\mu\text{m}$ . Patchy particles were formed by self-organization of the PS microspheres and PS homopolymers during the slow evaporation of toluene from the emulsion droplets at 100 °C for 7 h. Similarly, we prepared patchy particles with silica microspheres and PS homopolymers as follows. Silica microspheres in toluene (0.5 mL) were mixed with PS homopolymers dissolved in toluene (1 wt %, 0.5 mL) and the mixture was emulsified with 7 mL of aqueous Pluronic F108 solution (1 wt %) by homogenizing at 8000 rpm for 40 s. The demulsification and self-organization of silica particles and PS polymers were performed by heating the sample inside an oven at 60 °C for 3 h and subsequently at 80 °C for 1 h.

For patchy particles of PS microspheres and silica nanoparticles, 830 nm PS microspheres and 30 nm silica nanoparticles were dispersed in toluene at concentrations of 0.9 and 0.2 wt %, respectively. The same weight fractions were used to generate composite particles of PS microspheres and Au nanoparticles using 4 nm gold particles dispersed in toluene.

Because of the nonuniform size distribution of the emulsion droplets, the number of the encapsulated PS microspheres in the toluene droplets was widespread. Consequently, the self-organized binary clusters from a single experiment showed a full structural spectrum of composite or patchy particles.

For a demonstrative purpose, we also used monodisperse emulsion droplets as confined geometries for producing composite particles of PS microspheres and silica nanoparticles. To generate monodisperse toluene droplets in water, we used a shearing apparatus equipped with a Couette flow cell (PG398 type, TSR Co.), which was originally developed by Zerrouki et al.<sup>13</sup> In doing this, first, the cross-linked amidine PS microspheres (5 wt %) together with silica nanoparticles (0.2 wt %) were redispersed under sonication and stirring in toluene. The binary dispersion in toluene was then emulsified into an aqueous solution containing 1 wt % Pluronic F108 and 30 wt % polyvinylpyrrolidone (PVP K-90, Aldrich) by progressive mixing. The content of the dispersed phase (polystyrene/silica/toluene) was 25 wt % with respect to the total amount of the dispersed and continuous phases. The PVP K-90 was added to increase the viscosity of the continuous aqueous phase. The crude toluene-in-water emulsion droplets were polydisperse, and for unimodal size distribution, the crude emulsion was injected into a Couette flow cell at a rate of 0.7  $\mu\text{m/s}$  and sheared at a strain rate of 4167.85  $\text{s}^{-1}$  between two concentric cylinders with a gap distance of 100  $\mu\text{m}$ . The sheared monodisperse toluene-in-water emulsion droplets were heated at 60 °C for 2.5 h to remove toluene by evaporation, which induced the self-organization of PS microspheres and silica nanoparticles into composite particles. The composite particles were washed twice by centrifugation at 4000 g for 30 min and redispersion in aqueous Pluronic F108 solution (1 wt %) to remove PVP K-90 from the aqueous suspension.

**Density Gradient Centrifugation of Patchy or Composite Particles.** The density gradient centrifugation of patchy particles composed of silica microspheres and PS homopolymers was performed using the linear density gradient of glycerol (20–60%). A two-jar type gradient forming device was used to make linear gradient of glycerol inside a glass tube (50 mL). Next, 1.5 mL of a patchy particle suspension was loaded on the top level of the gradient. Centrifugation was performed at mild condition (600 rpm for 15 min) to obtain the fractionated bands from the sample.

Ultracentrifugation of the composite particles of PS microspheres and silica nanoparticles in a linear density gradient medium of polysaccharide (Ficoll 400, Aldrich) was performed to fractionate the composite particles according to the number of the PS microspheres. A gradient-forming device was used to make 2.9–10.5 wt % linear density gradient of polysaccharide inside a glass tube (10 mL). Next, 0.3 mL of the particle dispersion was carefully loaded on the top part in the glass tube, which contained 11 mL of the gradient solution. Finally, ultracentrifugation using a swing-bucket rotor at an acceleration of 3700 $\times$  gravitational acceleration for 20 min fractionated the composite particles into a few bands. Composite particles in each band contained an equal number of the constituent PS microspheres. The fractionated composite particles were taken out from each band by a syringe with blunt needle. These fractionated uniform clusters were washed by repeated centrifugation and redispersion several times to remove the gradient maker of polysaccharide for clear SEM imaging without any contaminants.

**Sample Characterization.** Electron microscopic images were taken under the field emission scanning electron microscope (FE-

(12) (a) Lauga, E.; Brenner, M. P. *Phys. Rev. Lett.* **2004**, *93*, 238301. (b) Schnall-Levin, M.; Lauga, E.; Brenner, M. P. *Langmuir* **2006**, *22*, 4547.

(13) (a) Zerrouki, D.; Rotenberg, B.; Abramson, S.; Baudry, J.; Goubault, C.; Leal-Calderson, F.; Pine, D. J.; Bibette, J. *Langmuir* **2006**, *22*, 57. (b) Mabile, C.; Leal-Calderson, F.; Bibette, J.; Schmitt, V. *Europhys. Lett.* **2003**, *61*, 708.



SEM, XL305FEG, Philips) or transmission electron microscope (F20, Tecnai). The patchy or composite particles in aqueous dispersion were separated from the dispersion medium by sedimentation for several days to remove the supernatant containing the excess amount of emulsion stabilizer, Pluronic F108, for clear SEM observation. The patchy or composite particles were then redispersed in fresh deionized water. The samples for SEM imaging were prepared by drying these aqueous dispersions of patchy or composite particles on a clean glass substrate at room temperature. After the drying process, the substrate with samples was attached to an aluminum holder with carbon tape and coated with gold by sputtering for SEM imaging. The same drying procedures were performed for TEM imaging by using a TEM grid instead of a glass substrate. The elemental compositions of the composite particles were analyzed by energy dispersive spectroscopy (EDS) equipped with an environmental electron microscope (E-SEM, LEO 1455VP). The samples for EDS were prepared by drying the particle dispersion on an aluminum holder without using carbon tape and glass substrate in order to detect carbon, oxygen, and silicon solely from the PS–silica composite particles.

**Surface Evolver Simulation.** Morphologies of patchy or composite particles were predicted by Surface Evolver simulation, a modeling program of liquid interfaces shaped by various forces and constraints.<sup>14</sup> The PS microspheres were modeled as liquid droplets in which the surface tension was an order of magnitude larger than the interfacial tension between toluene and water.<sup>12</sup> This high surface tension prevented the microspheres from deforming during simulation. These PS microspheres were bound to the interface of a toluene-in-water emulsion droplet. The contact angle at the microspheres bound to the toluene–water interface was fixed at a constant value. During computation, the total surface energy of the toluene–water interface, toluene–microsphere contact surface, and water–microsphere contact surface was minimized together with the hardcore repulsion between the microspheres. The initial positions of the microspheres on the emulsion droplet were used as an input parameter, and the volume of the droplet decreased slowly at a controlled rate during simulation. As the droplet volume was decreased, the microspheres rearranged to a new equilibrium configuration that minimized the sum of the total surface energy and the hardcore repulsive potential. Here, the drop phase contained the initially nanosized second component such as polymer chains or nanoparticles in addition to much larger PS microspheres. Therefore, the liquid volume of the droplet was not depleted completely during iterative computation but continued to decrease until the volume reduced to some fixed value, which was related to the excluded volume of the nanosized second component. The final interface shape predicted by Surface Evolver simulation provided an equilibrium configuration of patchy or composite particles. Especially the configurational evolution of the microspheres in a shrinking emulsion droplet containing nanosized particles was represented effectively from the numerical evolution of the second moment as a function of the volume of the target droplet during simulation.

When silica nanoparticles or polymers are dispersed together with PS microspheres in the toluene droplets in water, the emulsion droplets behave in a slightly different way compared to pure toluene-in-water emulsion droplets, which do not contain a nanosized second component. This is because the nanosized second component inside toluene droplets may change the contact angle of the toluene–water interface on the PS microspheres. According to Surface Evolver simulation, the change of contact angle does not affect the final morphologies of PS microclusters without any

second component inside droplets.<sup>14a</sup> However, when a nanosized second component is present in toluene droplets, the shape of binary colloidal clusters depends on the contact angle because the curvature of the toluene–water interface determines the surface curvature of the packed second component at the spaces between the PS microspheres. In this study, we compared Surface Evolver simulation results with experimental results for two different second components, namely, silica nanoparticles and PS polymers, both of which modified the contact angle to different degrees. The contact angle was determined from the simulation results, which gave the best-fit morphologies as compared with the SEM images. The resulting best-fit contact angles were 20 and 45° with silica nanoparticles and PS polymers as second components, respectively.

## Results and Discussion

**Patchy Particles.** We prepared patchy particles using PS homopolymer ( $M_w = 9100$  g/mol) as a second component in toluene droplets that contained 830 nm cross-linked PS microspheres. Toluene containing binary colloids was emulsified in water and self-organized by the slow evaporation of toluene. The colloidal PS microspheres were strongly bound at the interface of water and toluene by surface tension, whereas the PS homopolymers were completely dissolved in toluene, which was a good solvent for PS homopolymers. Therefore, as toluene was evaporated slowly, the colloidal particles were approaching together along the interface and formed clusters when toluene was completely removed. Meanwhile, the free polymers inside the toluene droplets filled and were consolidated in the interstices between the PS microspheres. Because toluene was a good solvent for PS homopolymers, the radius of gyration ( $R_g$ ) of PS homopolymers of molecular weight  $M_w$  in toluene can be estimated from the following relationship between  $R_g$  and  $M_w$ <sup>15</sup>

$$R_g \propto M_w^v$$

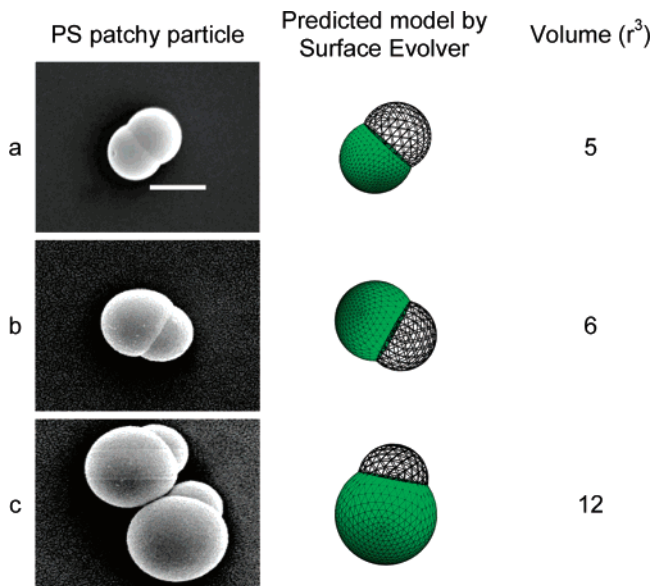
Here,  $v$  ( $\approx 3/5$ ) is the Flory exponent for good solvents. Thus, the radius of gyration of PS homopolymers used in our experiment was about 2.86 nm, implying that the polymeric second component acted as organic nanoparticles dispersed in toluene.

Figure 2 shows the representative SEM images of PS patchy particles for  $n = 1$ . In this case, only one patch was formed on a PS microsphere and the resulting patchy particle had either a symmetric shape (Figure 2a) or nonsymmetric snowmanlike structures (parts b and c in Figure 2), the shapes of which were similar to the colloidal snowman particles synthesized by Okubo and his colleagues.<sup>16</sup> The structural symmetry was dependent on the volume of the PS homopolymers relative to the PS microsphere. The morphologies of the patchy particles in Figure 2a–c were also predicted by Surface Evolver.<sup>12,14</sup> In Surface Evolver simula-

(14) (a) Brakke, K. A. *Exp. Math.* **1992**, *1*, 141. (b) <http://www.susqu.edu/facstaff/b/brakke/evolver/>.

(15) (a) Berry G. C. *J. Chem. Phys.* **1966**, *44* (12) 4550. (b) Hennequin, Y.; Evens, M.; Quezada Angulo, C. M.; van Duijneveldt, J. S. *J. Chem. Phys.* **2005**, *123*, 054906.

(16) (a) Okubo, M.; Yamashita, T.; Minami, H.; Konishi, Y. *Colloid Polym. Sci.* **1998**, *276*, 887. (b) Okubo, M.; Wang, Z.; Ise, E.; Minami, H. *Colloid Polym. Sci.* **2001**, *279*, 976. (c) Minami, H.; Wang, Z.; Yamashita, T.; Okubo, M. *Colloid Polym. Sci.* **2003**, *281*, 246. (d) Okubo, M.; Fujibayashi, T.; Yamada, M.; Minami, H. *Colloid Polym. Sci.* **2005**, *283*, 1041.



**Figure 2.** Scanning electron micrographs of the PS patchy particles for  $n = 1$  generated from PS microspheres and PS homopolymers. Scale bar is  $1 \mu\text{m}$ .

tion, the contact angle at the PS microspheres bound to the toluene–water interface was fixed at  $45^\circ$ . As the amount of the PS homopolymers in an emulsion droplet was increased from  $5r^3$  to  $12r^3$ , in which  $r$  was the radius of the PS microsphere, the morphologies of snowmanlike patchy particles were quite similar to those of experimentally observed patchy particles, as displayed in Figure 2a–c.

The structure evolution for the case of  $n = 2$ , shape-anisotropic particles such as peanut-shaped and football-like structures were formed depending on the amount of the PS homopolymers, as shown in images a and b of Figure 3. The initial positions of the PS microspheres on the interface of an emulsion droplet also affected the final morphology of the patchy particle. For  $n = 2$ , we observed three different structures as displayed in Figure 3b–d. The two microspheres embedded in the patchy particle were separated and a symmetrical football-like patchy particle as displayed in Figure 3b was created when the microspheres were positioned on the opposite sides on the emulsion droplet. However, V-shaped patchy particles as shown in images c and d of Figure 3 were formed when the two PS microspheres were located on the same hemisphere of an emulsion droplet in the initial stage. This implies that the initial configuration of the microspheres influenced the structure of the patchy particle in addition to the volume of the PS homopolymers contained in an emulsion droplet. In Figure 3e, the morphologies of the patchy particles were also predicted by Surface Evolver by varying the initial positions of two PS microspheres on the interface of the emulsion droplet. In Figure 3e, the second moment of two microspheres bound to an emulsion droplet and the corresponding morphology were shown as a function of the emulsion volume ( $V_E$ ). As noted, the numerical simulation predicted both the experimentally observed football-like and V-shape patchy particles. If the nanoscale second component of PS homopolymers was not included in the emulsion droplets, all of patchy particles with two microspheres would be

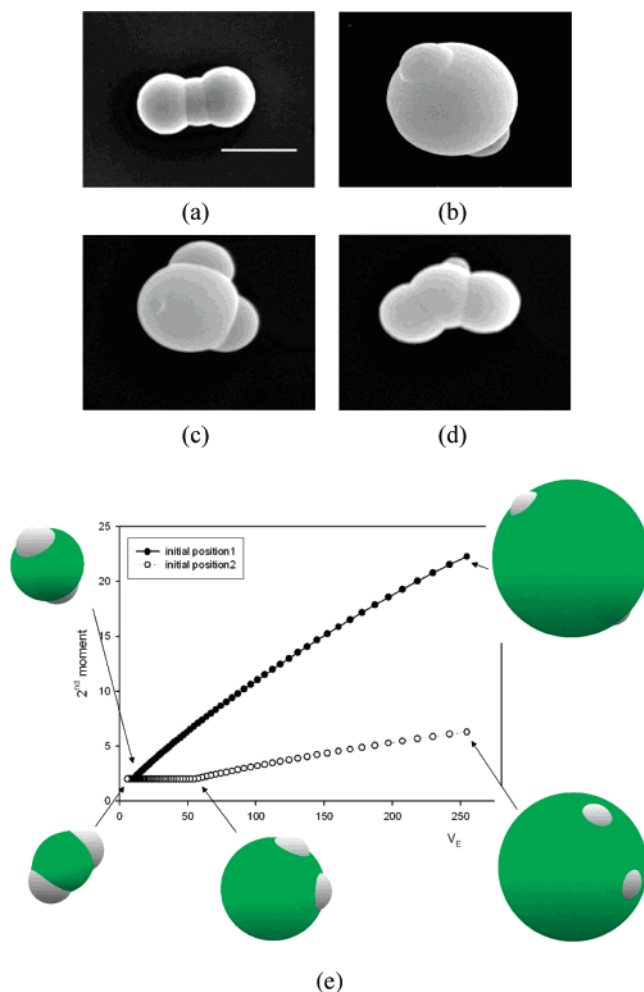


**Figure 3.** (a–d) Scanning electron micrographs of the PS patchy particles for  $n = 2$ . Scale bar is  $1 \mu\text{m}$ . (e) Surface Evolver simulation for changes in the numerical second moments of the PS microspheres trapped in emulsion droplets as a function of the emulsion volume ( $V_E$ ) for  $n = 2$ .

structured into dimers in line alignment regardless of the initial configuration.

As shown in Figure 4 for  $n \geq 3$ , trimer, tetramer, pentamer, hexamer, and higher-order clusters of the PS microspheres were partially covered with PS homopolymers. For  $n = 5$ , the PS microspheres were packed into a triangular dipyrmaid as shown in the SEM images of Figure 4a. The minimal second moment clusters of the PS microspheres, which had been formed in the absence of the nanosized second component in our previous study, were reproduced regardless of the presence of the linear homopolymers when the amount of encapsulating polymer was sufficiently small.<sup>6</sup> As we shall see shortly, when a large amount of the nanoscale second component was included in toluene emulsion droplets, a small fraction of the composite particles was not structured into the minimal second-moment configurations. In the final stage of the cluster formation, a capillary force at the toluene–water interface pulled the PS homopolymers into the valleys between the large PS microspheres, as in Figure 4a. All the edges of PS microspheres were not covered by the PS homopolymers, as shown in the SEM images of Figure 4a. When the size of the emulsion droplets was large enough to contain a larger number of the PS microspheres and large volume of the PS homopolymers, the PS supraballs

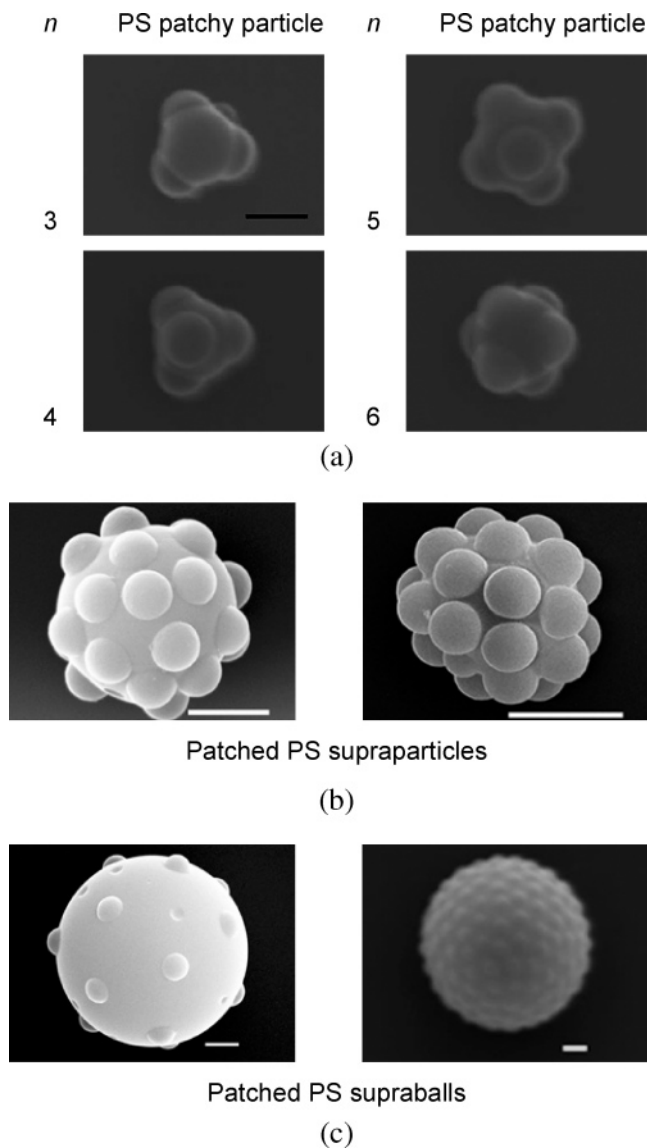
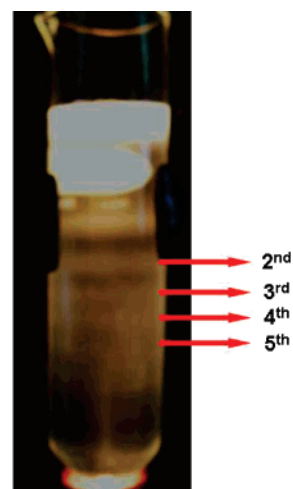


**Figure 4.** (a, b) Scanning electron micrographs of the PS patchy particles generated using the PS microspheres and PS homopolymers. Scale bars are  $1\ \mu\text{m}$ . (c) Scanning electron micrographs of the patched PS supraballs when the volume of the PS homopolymers is greater than  $V_c$ . Scale bars are  $1\ \mu\text{m}$ .

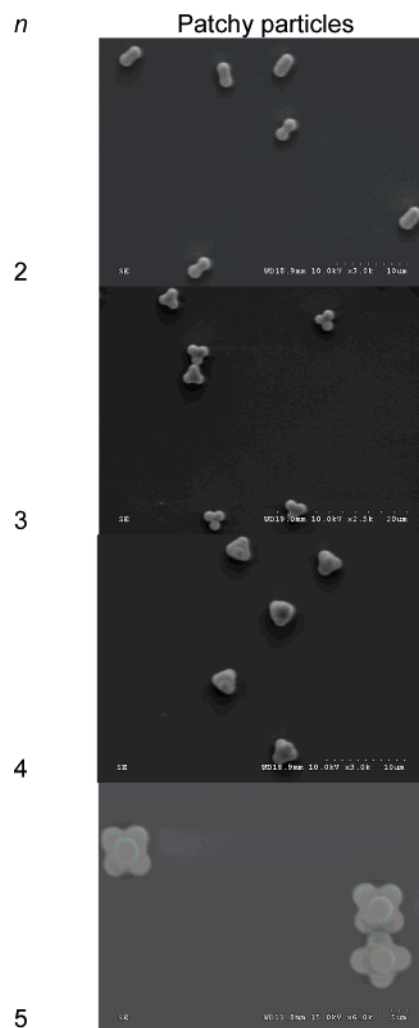
with surface patterns were generated as shown in Figure 4b. Similar supraballs have been produced by stress-driven self-assembly of Ag core and  $\text{SiO}_x$  shell.<sup>17</sup>

As we discussed in our previous report, the packing process of the microspheres were governed by capillary force at interface.<sup>3</sup> As toluene evaporated, the PS microspheres were touching together, forming a critical packing, and they were then rearranged rapidly as toluene evaporated further.<sup>12</sup> Suppose that the volume of the emulsion droplet at the critical packing is  $V_c$  in the absence of the PS homopolymers. When the volume of the PS homopolymers in the emulsion droplet is larger than  $V_c$ , the critical packing of the PS microspheres is not achievable because the emulsion volume cannot be smaller than  $V_c$  by evaporation. In this case, the PS microspheres were embedded in the PS homopolymer balls and separated each other as shown in Figure 4c.

(17) Li, C.; Zhang, X.; Cao, Z. *Science* **2005**, *309*, 909.



(a)

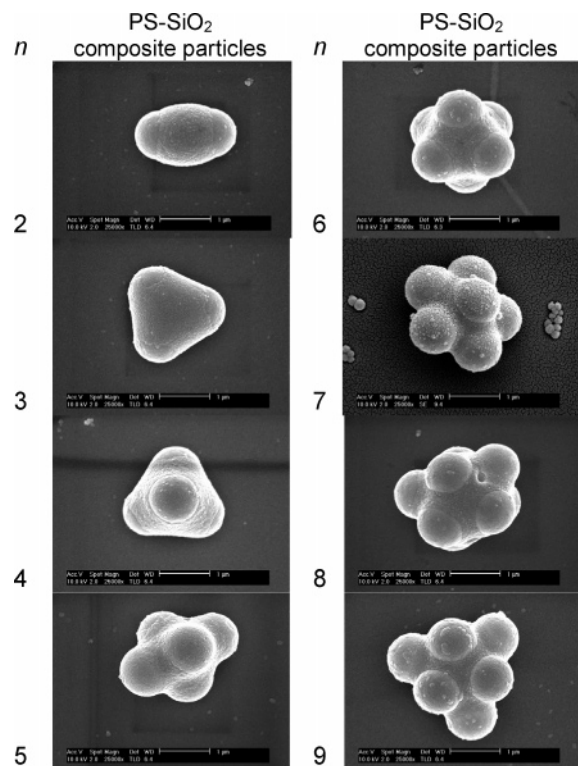


(b)

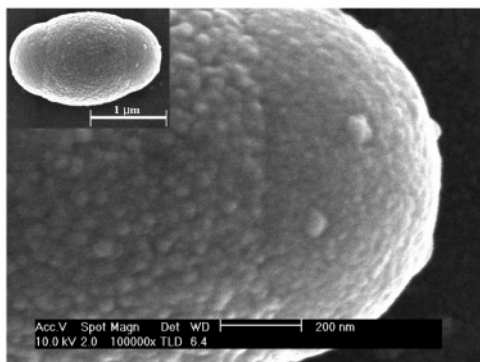
**Figure 5.** (a) Test tube containing patchy particles of silica microclusters encapsulated with PS homopolymers separated by density gradient centrifugation and (b) SEM images of patchy particles taken from each band. Scale bars are  $10\ \mu\text{m}$ .

Sometimes the surface pattern of the embedded PS microspheres inside the patched PS supraballs were quite regular and ordered, as shown in Figure 4c.





(a)



(b)

**Figure 6.** (a) Scanning electron micrographs of the composite particles of the PS microspheres and silica nanoparticles. (Scale bars are 1  $\mu\text{m}$ .) (b) High-magnification scanning electron micrographs of the composite particles of the PS microspheres and silica nanoparticles for  $n = 2$ . Scale bar is 200 nm.

Patchy particles of silica microspheres encapsulated with PS homopolymers were also generated to demonstrate that the density gradient centrifugation could fractionate the patchy particles according to the number of silica microspheres. Because the contribution of the encapsulating PS homopolymers to the specific gravity of these patchy particles were relatively negligible compared to silica microspheres, we chose the silica microspheres/PS homopolymers as another model system for the density gradient centrifugation of the patchy particles. This is because the encapsulating PS homopolymer is light relative to silica microspheres. Thus, we applied a linear density gradient of glycerol, which was used for the fractionation of silica microclusters in our previous report.<sup>7</sup> Figure 5a shows the fractionation result of the sample, which contains at least five separated bands from the top. Thus, by taking out the patchy particles from each

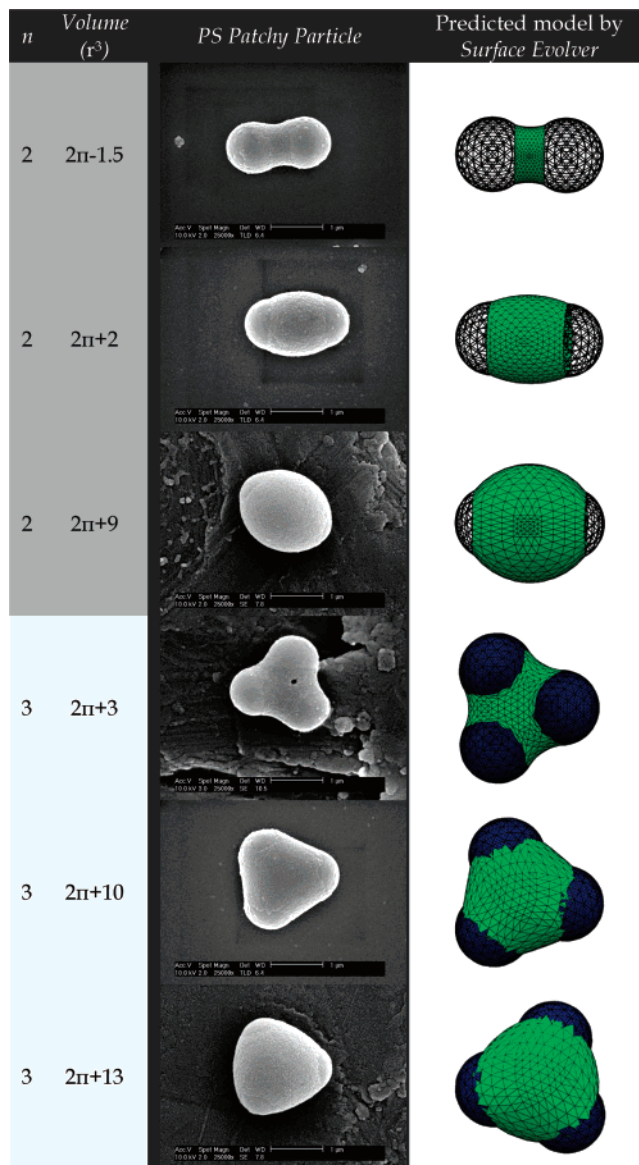


**Figure 7.** Experimentally observed structural evolution of the PS-silica composite particles for  $n = 2$  and 3 and the structures predicted by Surface Evolver. Scale bars are 1  $\mu\text{m}$  and  $r$  indicates the radius of the PS microsphere.

band, we could produce all identical patch particles of dimers, trimers, and tetramers, as shown in Figure 5b. Dimers ( $n = 2$ ) and tetramers ( $n = 4$ ) are of practical significance as building blocks of novel colloidal photonic crystals with diamond lattice that possess full and robust photonic band gaps. Recently, Manoharan et al. used a 10 mL test tube to fractionate colloidal clusters and obtained billions ( $1 \times 10^8$  to  $1 \times 10^{10}$ , or 0.1 to 10 mg) of all identical clusters from each band.<sup>6</sup> In our work, we used 50 mL test tubes and produced patchy particles in macroscopic quantities from each band up to ( $n = 5$ ).

Although higher-order patchy particles ( $n > 4$ ) were produced, it was practically difficult to obtain all identical higher-order patchy particles because of the difficulty in taking out the samples from the bands in the bottom without disturbing the bands. Therefore, we carefully examined the structures of higher-order patchy particles through SEM and found some patchy particles with weird structures that did not minimize the second moments. These particles were

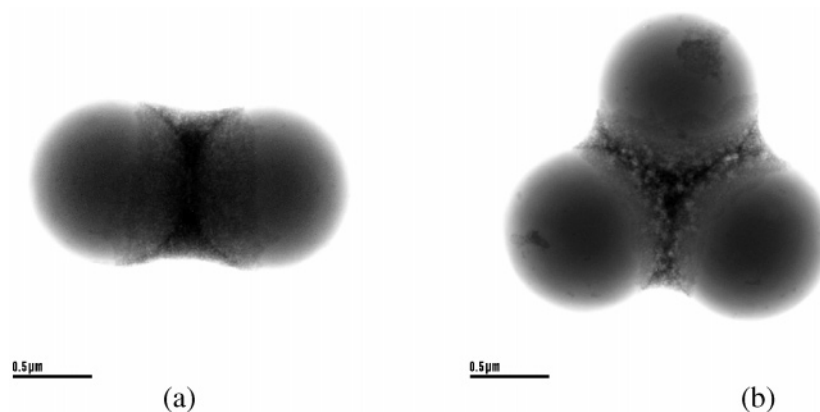


**Figure 8.** Transmission electron micrographs of the composite particles of the PS microspheres and silica nanoparticles for  $n = 2$  and 3. Scale bars are 500 nm.

marked with red circles in Figure S3b of the Supporting Information. The fraction ( $\phi$ ) of patchy particles with nonminimal second-moment configurations was increased gradually with the number ( $n$ ) of the constituting microspheres for  $4 < n < 12$ . For example,  $\phi$  was about 10% for  $n = 5$  and 15% for  $n = 6$ . Overall, the number averaged fraction ( $\phi$ ) of such patchy particles was about 25% for  $4 < n < 12$ .

The origin of the patchy particles with nonminimal second-moment structure can be explained as follows. First, when a large amount of PS homopolymers was present together with silica microspheres in toluene drops, the solvent toluene would be evaporated completely before the silica microspheres could be packed into the spherical close packing. This was especially true if the initial arrangement of the microspheres was far away from the spherical symmetric distribution. The spherical close packing is the essential step for the rearrangement of the microspheres toward the minimal second moment structures. This was shown experimentally and numerically for dimeric patchy particles in Figure 3. Second, the presence of PS homopolymers induced the depletion interaction and aggregated the microspheres during evaporation of toluene, which was also responsible for the formation of the patchy particles with weird structures.

**Composite Particles.** As shown in the TEM images of Figure S4 in the Supporting Information, organo-silica nanoparticles dispersed in toluene were about 30 nm in diameter with narrow size distribution. These silica nanoparticles dispersed in toluene were mixed with the crosslinked 830 nm PS microspheres and the mixture dispersion was emulsified into toluene droplets in water. Composite particles of the PS microspheres and silica nanoparticles were formed after toluene was removed by evaporation. The elemental compositions of the PS–silica composite particles were confirmed with energy-dispersive spectroscopy, as shown in Figure S5a of the Supporting Information. From the spot analysis of the sample, the peaks in the EDS spectra for carbon, oxygen, and silicon from PS clusters and silica shells of the composite particles can be clearly observed, as shown in Figure S5a of the Supporting Information. However, when EDS analysis was performed for the spot without samples, only aluminum, magnesium, and gold peaks were observed because of the aluminum holder and gold coating, as shown in Figure S5b of the Supporting information. This controlled

analysis provided clear evidence for the existence of the elemental compositions such as carbon, oxygen, and silicon of the composite particles with patches.

The configurations of the PS microspheres in the composite particles were shown in Figure 6a. In the final stage of the evaporation-induced clustering, the toluene phase formed menisci around the valleys between the large microspheres, and a capillary force pulled the small silica nanoparticles into the valleys. The composite particles were not fully covered by silica nanoparticles forming coordinated patches near the edges as shown in the highly magnified SEM image in Figure 6b.

During the evaporation of toluene droplets, the emulsion stabilizer (Pluronic F108) was adsorbed on the surface of PS microspheres, especially on the patches that were not covered with silica nanoparticles in toluene droplet. Because the cross-linked PS microspheres tended to swell in toluene, further heating to remove the residual toluene inside microspheres after clustering resulted in the penetration of hydrophobic block of Pluronic F108 inside the microspheres.<sup>18</sup> Because our composite particles have patches of PS that were not coated with silica nanoparticles, the hydrophilic blocks of Pluronic F108 were permanently anchored only on the PS patches, causing the steric repulsion between the composite particles in aqueous dispersion. Meanwhile, Pluronic F108 molecules that were adsorbed physically on the surface of silica-coated parts of the composite particles were removed by the washing process.

As shown in Figure 7, the structure evolutions of the composite dimers ( $n = 2$ ) and trimers ( $n = 3$ ) were predicted by Surface Evolver, in which the amount of the silica nanoparticles was changed as an adjustable parameter. The contact angle between toluene and aqueous phase on the PS microspheres was fixed at  $20^\circ$  in this calculation. As the amount of the silica nanoparticles was increased, the morphologies of dimers and trimers were changed as noted in Figure 7 and those predicted shapes coincided well with those of the experimentally observed composite clusters. For the PS–silica composite clusters, Surface Evolver simulation predicted the experimentally observed shapes successfully with a lower contact angle at  $20^\circ$  than at  $45^\circ$  for the PS–

(18) Kim, A. J.; Manoharan, V. N.; Crocker, J. C. *J. Am. Chem. Soc.* **2005**, *127*, 1592.



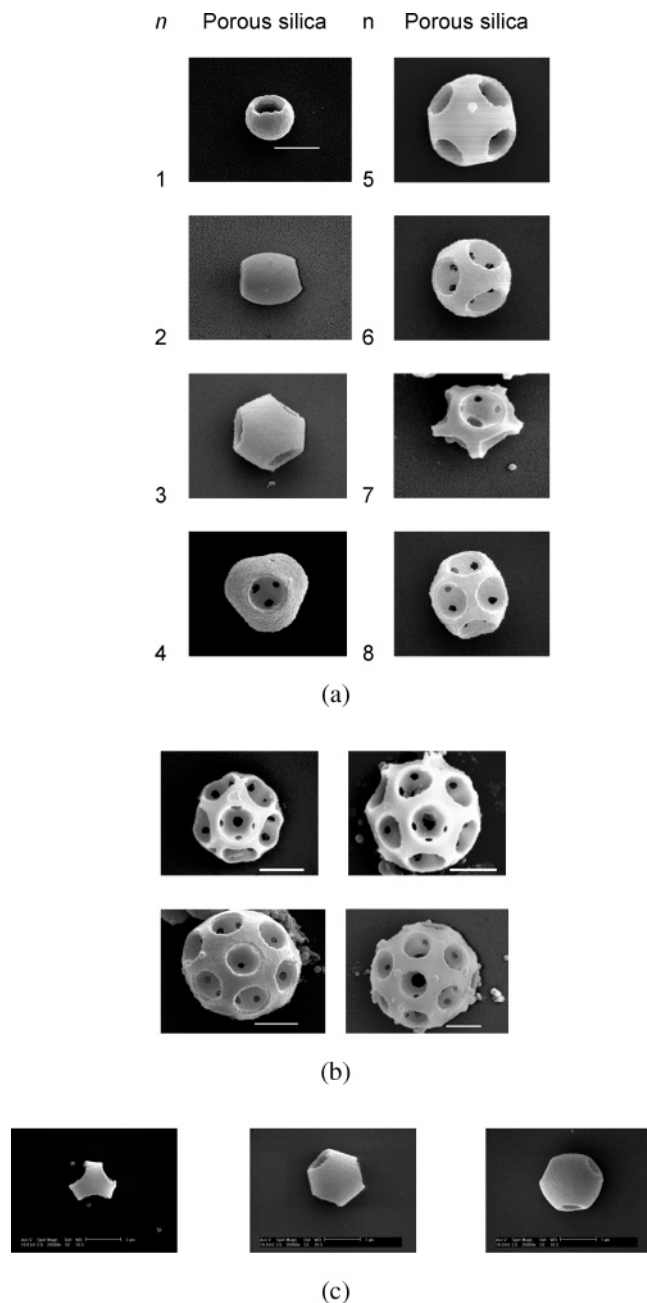


**Figure 9.** (a) Scanning electron micrographs of the porous silica particles produced by burning out the PS microspheres from the composite particles. Scale bar is 1  $\mu\text{m}$ . (b) Cage-like porous silica particles. Scale bars are 1  $\mu\text{m}$ . (c) Structural evolution of the porous silica for  $n = 3$ . Scale bars are 1  $\mu\text{m}$ .

silica composite clusters. This low contact angle on the PS microspheres reflected the high affinity between the hydrophobic silica nanoparticles and the cross-linked hydrophobic PS microspheres. The TEM images of Figure 8 showed that our composite particles for  $n = 2$  and 3 were partially covered with the silica nanoparticles and no silica shells were formed in the outer edges of the composite clusters.

Figure 9a shows the hollow silica particles that were produced by burning out the PS microspheres from the silica-PS composite clusters at 500  $^{\circ}\text{C}$  for 5 h. Because the outer edges of the microspheres were not covered with the silica nanoparticles, large well-coordinated windows were formed after removal of the PS microspheres. Figure 9b shows the higher-order hollow silica clusters that resembled

the cage-like hollow polymeric particles produced by Zhang and his colleagues.<sup>19</sup> These hollow silica architectures can be used as catalytic supports, filters, and light diffusers for infrared wavelengths.<sup>20</sup> Figure 9c contains the structure evolution of the silica skeleton for  $n = 3$  as the amount of silica nanoparticles was increased in a toluene-in-water droplet.

We also produced gold-PS composite particles by using gold nanoparticles instead of the silica nanoparticles. As expected, the outer edges of the PS-Au composite particles were not covered with the gold nanoparticles as shown in Figure 10a. For gold shells with coordinated windows, we tried to burn out the organic parts from the PS-Au composite particles, but the structures were destroyed, leaving the crumbled aggregates of gold. This was because the melting point of 4 nm gold nanoparticles is lower than 500  $^{\circ}\text{C}$ .<sup>21</sup> In this work, the PS microspheres were removed using oxygen-reactive ion etching (RIE), which is a highly selective and gentle method. Although RIE is a low-yield process and requires additional equipment, it is much more effective for obtaining hollow structures than calcination at high temperature, which could destroy the metallic nanostructures. Figure 10b displays hollow gold structures prepared by  $\text{O}_2$  RIE for 25 min. Such gold-shell particles are potentially useful for catalysts with highly efficient mass-transfer rates. The effectiveness of the hollow gold architectures for this application can be found more clearly from the aggregates of PS and gold nanoparticles with unusual complexity for large  $n$ , as shown in Figure S6 of the Supporting Information. Also important to note is that these types of hollow architectures can be produced using gold and metal oxide nanoparticles as shells and PS microspheres as sacrificial templates to make the surface structures of the hollow particles different in atomic level for catalysis applications.<sup>22</sup>

Thus far, we have demonstrated useful and facile method for producing various types of patchy or composite particles from polydisperse emulsion droplets in size. Obviously, the encapsulated amount of the nanosized second component is proportional to the size of emulsion droplets. Consequently, various types of patchy or composite particles can be produced in a single batch of the sample in this experimental scheme. Indeed, we could observe most abundant structural features of patchy or composite particles as a function of the number ( $n$ ) of PS microspheres and the amount of nanosized second component. For example, the SEM image in Figure S7 of the Supporting Information shows the PS patchy particles of different numbers of PS microspheres with various amounts of PS homopolymers, which were produced from the same polydisperse toluene-in-water emulsion. Also, Figure S8a shows the PS-silica composite particles produced from polydisperse emulsion droplets. The variety of the morphology of the composite clusters for a given  $n$  was caused by the nonuniformity of the initial droplet size, which

(19) He, X. D.; Ge, X. W.; Liu, H. R.; Wang, M. Z.; Zhang, Z. C. *Chem. Mater.* **2005**, *17*, 5891.

(20) Klein, S. M.; Manoharan, V. N.; Pine, D. J.; Lange, F. F. *Langmuir* **2005**, *21*, 6669.

(21) Cortie, M. B. *Gold Bull.* **2004**, *37*, 12.

(22) Subramanian, V.; Wolf, E. E.; Kamat, P. V. *J. Am. Chem. Soc.* **2004**, *126*, 4943.

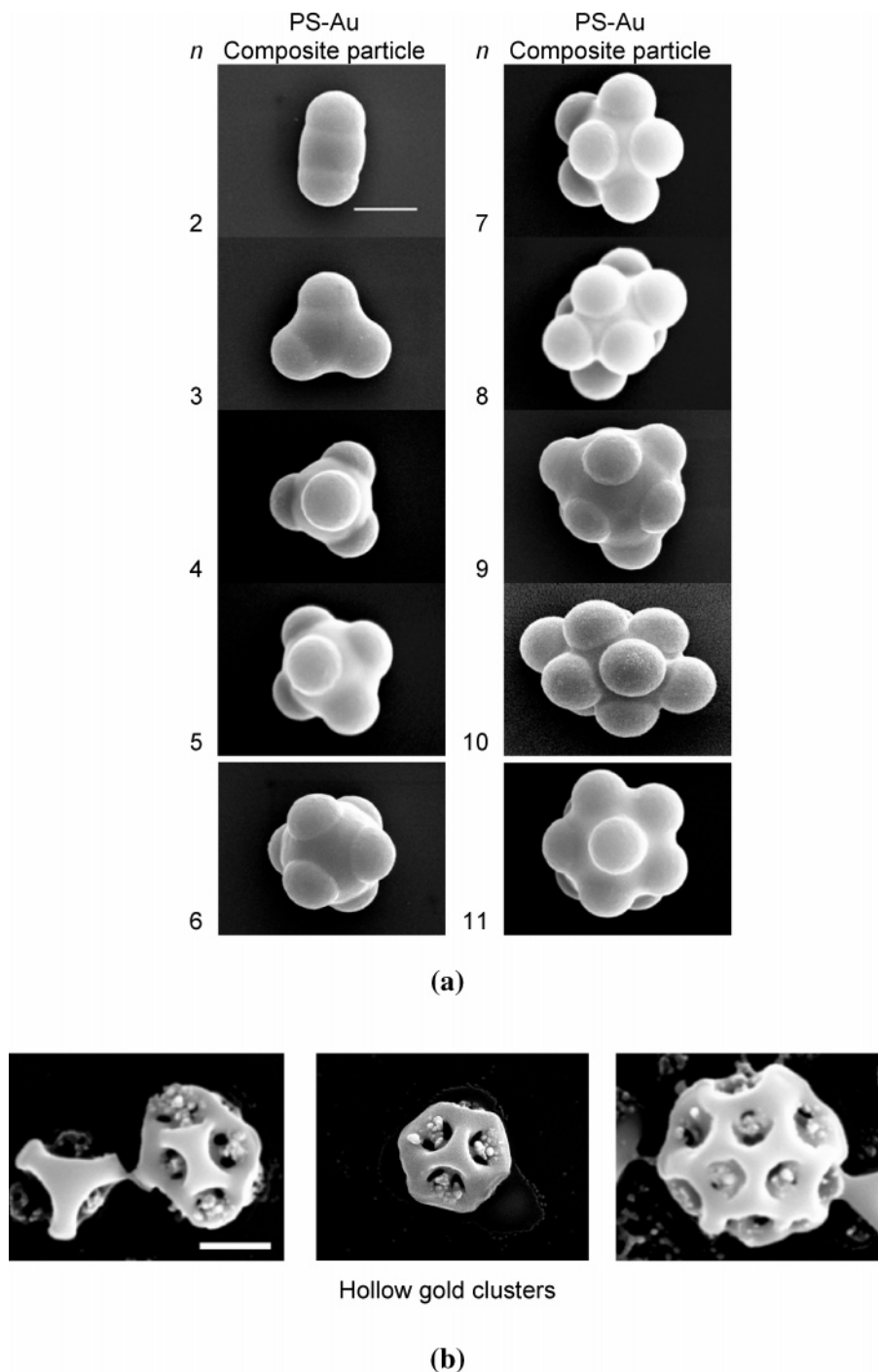


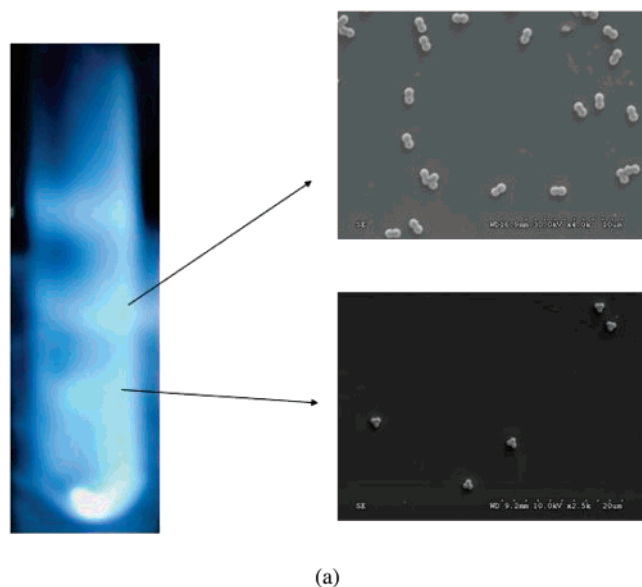
**Figure 10.** Scanning electron micrographs of the composite particles of (a) the PS microspheres and gold nanoparticles and (b) porous gold particles produced by etching out PS via RIE. Scale bars are 1  $\mu\text{m}$  in (a) and 500 nm in (b).

is proportional to the encapsulated volume of the nanosized silica particles. In Figure S8a, we can also observe small spherical nanospheres, which were probably produced from toluene-in-water emulsion droplets without PS microspheres. Indeed, as shown in Figure S8b, various types of hollow clusters were produced together with small nanospheres made of silica by heat treatment of the sample.

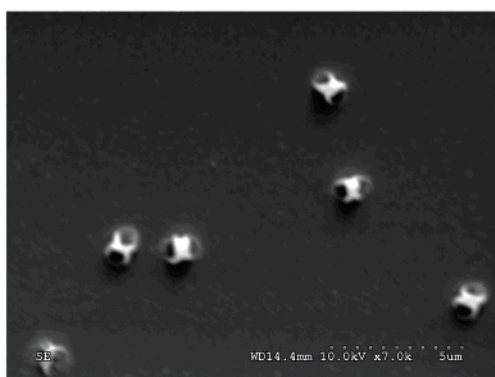
**Composite Particles from Monodisperse Emulsion Droplets.** For practical applications, we have to engineer the emulsification system for uniform and pure clusters. Recently, Zerrouki et al. synthesized large amount of silica colloidal clusters from relatively monodisperse oil-in-water emulsion droplets by shearing polydisperse emulsions be-

tween two concentric cylinders.<sup>13</sup> In addition, other useful methods using microfluidic devices, micropipette injection devices, and electrospray were demonstrated for generating monodisperse emulsion droplets.<sup>23</sup> Nevertheless, the number of large microspheres will fluctuate following Poisson distribution even in these engineered systems.<sup>24</sup> However,

(23) (a) Yi, G.-R.; Manoharan, V. N.; Micheal, E.; Elsesser, M. T.; Yang, S.-M.; Pine, D.-J. *Adv. Mater.* **2004**, *16*, 1205. (b) Yi, G.-R.; Thorsen, T.; Manoharan, V. N.; Hwang, M.-J.; Jeon, S.-J.; Pine, D. J.; Quake, S. R.; Yang, S.-M. *Adv. Mater.* **2003**, *15*, 1300. (c) Yi, G.-R.; Manoharan, V. N.; Klein, S.; Brzezinska, K. R.; Pine, D. J.; Lange, F. F.; Yang, S.-M. *Adv. Mater.* **2002**, *14*, 1137. (d) Moon, J. H.; Yi, G.-R.; Yang, S.-M.; Pine, D. J.; Park, S.-B. *Adv. Mater.* **2004**, *16*, 605.



(a)



(b)

**Figure 11.** (a) Test tube containing composite particles of PS microspheres and silica nanoparticles separated by density gradient centrifugation and SEM images of composite particles extracted from the second and third bands. (b) SEM image of the silica structures that were left behind after the PS microspheres were removed selectively from the second-order clusters. Scale bar is 5  $\mu\text{m}$ .

the morphology of patchy or composite particles will be uniform for a fixed number  $n$  of large microspheres, because the amount of nanosized second component is proportional mainly to the volume of the emulsion droplet for a given  $n$ . The clusters can then be fractionated subsequently according to  $n$  by the well-known techniques, i.e., density gradient centrifugation or flow cytometry.<sup>6,25</sup>

For demonstrative purposes, composite particles of PS microspheres and silica nanoparticles were prepared from quasi-monodisperse emulsion droplets using a Couette-type emulsifier developed by Zerrouki et al.<sup>13</sup> The Couette-type emulsifier was able to generate nearly monodisperse emulsion droplets. Therefore, the amounts of silica nanoparticles inside emulsion droplets were almost uniform, which led to the generation of composite particles with a uniform morphology for a fixed  $n$ . The drop size could be controlled by shearing rate and time, which in turn determined the

structure of the binary clusters. We tried to fractionate the composite particles generated from monodisperse emulsion droplets according to  $n$  by density gradient centrifugation. To do this, we followed the procedure reported by Manoharan et al.<sup>6</sup> Figure 11a shows that the composite particles of PS microspheres and silica nanoparticles were separated successfully into three isolated bands in linear density gradient centrifugation. As shown in the SEM images of Figure 11a, second- ( $n = 2$ ) and third-order ( $n = 3$ ) clusters of PS microspheres with silica nanoparticles were successfully fractionated by density gradient centrifugation. To confirm the existence of silica nanoparticles, we burnt out the second-order ( $n = 2$ ) composite clusters at 500  $^{\circ}\text{C}$  for 5 h, and the result is shown in Figure 11b. Indeed, the SEM image shows the resultant silica structures with hollow vacancies, which were left behind by thermally decomposed PS microspheres.

### Conclusions

We demonstrated a simple and unique method for preparing patchy or composite particles with coordinated patches or windows from polydisperse oil-in-water emulsions, in which PS or silica microspheres were dispersed together with linear homopolymers or nanoparticles in oil droplets. Specifically, in the presence of PS homopolymers, the clusters of the PS microspheres were covered partially with the PS homopolymers, leaving behind well-organized patches. Most of the patchy particles for  $n \leq 4$  had final configurations that minimized the minimal second moments of the constituting microspheres. However, small fractions of the patchy particles for  $4 < n < 12$  had nonminimal second-moment configurations due to the presence of the encapsulating PS homopolymers. The fraction of such patchy particles was increased gradually with the number of the constituting microspheres. The addition of small organo-silica or gold nanoparticles produced the organic-inorganic composite clusters with coordinated patches. In the latter case, the selective removal of the PS microspheres from the composite clusters produced the silica or gold shell particles with well-organized windows, which is of practical significance for various applications. Binary clusters were also generated from monodisperse emulsion droplets using Couette-type emulsifier and the resultant composite particles were fractionated to produce binary clusters with a uniform configuration.

**Acknowledgment.** This work was supported by a grant from the Creative Research Initiative Program of MOST/KOSEF for “Complementary Hybridization of Optical and Fluidic Devices for Integrated Optofluidic Systems.” The Korea Basic Science Institute is also acknowledged for allowing us to use EDS, SEM, and TEM equipment.

**Supporting Information Available:** SEM and TEM images of PS microspheres, silica, and gold nanoparticles; EDS spectra of the PS-silica composite clusters; SEM images of hollow gold architectures; and the representative SEM images of composite particles and heat treated structures. These materials are available free of charge via the Internet at <http://pubs.acs.org>.

(24) Hinds, W. C. *Aerosol Technology*, 2nd ed.; John Wiley & Sons: New York, 1998.

(25) Liddel, C. M.; Summers, C. J. *Adv. Mater.* **2003**, *15*, 1715.